

Contents lists available at ScienceDirect

# Combustion and Flame

journal homepage: www.sciencedirect.com/journal/combustion-and-flame



# Experimental study on expanding hydrogen/air turbulent premixed flames under high turbulence intensities

Jinzhou Li <sup>a,b</sup>, Huangwei Zhang <sup>b</sup>, Junfeng Yang <sup>a,\*</sup>

- <sup>a</sup> School of Mechanical Engineering, University of Leeds, Leeds LS2 9JT, United Kingdom
- <sup>b</sup> Centre for Hydrogen Innovations, National University of Singapore, 117580, Singapore

#### ARTICLE INFO

# Keywords: Turbulent hydrogen spherical flames Self-similar flame propagation High turbulence intensity Lewis number Flame propagation velocity correlation

#### ABSTRACT

This study measures the characteristics of expanding hydrogen/air premixed turbulent flames over a wide range of equivalence ratios,  $\phi$  (0.5 to 1.5) and root-mean-square (r.m.s) turbulent velocities, u' (1 m/s to 9 m/s), using a fan-stirred combustion vessel with high-speed schlieren imaging. These experimental conditions enable the exploration of both Lewis number and turbulence intensity effects on turbulent flame propagation in hydrogen/ air flames, addressing a research gap related to flame behavior under relatively high turbulent intensities (u' > 4m/s). Pressure oscillations were observed after peak pressure when u' exceeded 5 m/s, with their amplitude increasing with increasing u'. Hydrogen/air mixtures with lower effective Lewis numbers, Leeff exhibited enhanced turbulent flame acceleration compared to those with higher Leeff, as indicated by the increase in the normalized turbulent flame propagation speed  $(S_{sch}/S_s)$  with decreasing  $Le_{eff}$  across all flame radii. The influence of Lewis number on turbulent flame acceleration diminished when Leeff large than unity. The scaling of these normalized turbulent flame speeds with the Reynolds number,  $Re_T$  followed a power-law trend, with improved correlation when  $Re_T$  was normalized by  $Le_{eff}$ . The mean representative flame propagation velocity,  $\overline{u}_{\overline{c}=0.5}$ determined for flame radii between 15 mm and 50 mm, increased with both  $\phi$  and u', reaching a maximum of approximately 27 m/s at  $u^{\prime}=9$  m/s and  $\phi=1.5$ . Based on the present experimental data and existing literature on hydrogen/air flames, two correlations are proposed to cover a wide range of Leeff and u'. One is correlated with the Karlovitz stretch factor, K and the other with turbulent flame Reynolds number normalized by effective Lewis number  $(Re_T/Le_{eff})$  both showing excellent agreement with the data, with  $R^2$  values of 0.95.

# 1. Introduction

Hydrogen has emerged as an effective energy carrier, drawing attention for its advantages, including zero carbon emissions, high laminar burning velocity, broad flammability range, and high mass-based heating value, making it highly attractive for clean energy applications [1]. As a carbon-free fuel, hydrogen may play a crucial role in decarbonizing power sector, especially in internal combustion (IC) engines [2,3] and gas turbines [4,5]. Despite its benefits, hydrogen's high reactivity also presents safety challenges, especially the risk of deflagration-to-detonation transition (DDT), which is a critical explosion scenario [6]. Thus, understanding the fundamental combustion characteristics of premixed hydrogen flames is essential for its deployment in combustion engines, gas turbines, and risk assessment.

Extensive studies [7-10] have been conducted to measure the key

characteristics of laminar premixed hydrogen flames, such as laminar burning velocity [7–10], Markstein length/number [7–9], and cellular instability [8,9] over a wide range of temperatures, pressures, and/or equivalence ratios. However, understanding laminar flame behavior alone is insufficient for evaluating the combustion stability of hydrogen in practical systems, such as combustion engines and gas turbines, as most combustion and explosion events occur under turbulent conditions. Unlike laminar flames, turbulent flames interact with turbulent eddies that may distort and wrinkle the flame front, thereby increasing its surface area. The increased flame surface area enhances the burning rate and hence leads to accelerated flame propagation. It is essential to study the hydrogen combustion in turbulent flows to advance hydrogen utilization in realistic energy systems.

Turbulent premixed hydrogen flames in fan-stirred combustion vessels have been investigated [11–14]. For instance, Goulier et al. [11] measured turbulent hydrogen/air flames at root-mean-square turbulent

E-mail address: J.Yang@leeds.ac.uk (J. Yang).

<sup>\*</sup> Corresponding author.

Nomenclature			unstretched laminar flame speed (m/s) time (s)			
а	empirical correction factor	T	temperature (K)			
Α	flame surface area (m <sup>2</sup> ); mixture strength factor	$T_{ad}$	adiabatic flame temperature (K)			
$\overline{c}$	mean progress variable	$T_u$	unburnt temperature (K)			
Da	Damköhler number, $Da = (L/u')(\delta_l/u_l)$	Ü	mean flow velocity (m/s); ratio of $u_t/u_k$			
f	fan speed (rpm)	u′	root-mean-square turbulent velocity (m/s)			
K	Karlovitz stretch factor, $K = (u'/\lambda)(\delta_l/u_l)$	$u_l$	unstretched laminar burning velocity (m/s)			
Ka	Karlovitz number, $\left(\frac{\delta_L}{\eta}\right)^2$	$u_t$	turbulent burning velocity (m/s)			
κα	( ' /	$u_{t,\overline{c}=0.5}$	turbulent burning velocity at $\overline{c} = 0.5$ (m/s)			
L	integral length scale of combustion vessel (20 mm)	$u_{\overline{c}=0.5}$	representative flame propagation velocity at $\overline{c} = 0.5$ (m/s)			
$Le_{e\!f\!f}$	effective Lewis number	$\overline{u}_{\overline{c}=0.5}$	mean representative flame propagation velocity, evaluated			
$Le_D$	Lewis numbers of the deficient reactant		over $r_{sch} = 15-50 \text{ mm (m/s)}$			
$Le_E$	Lewis numbers of the excess reactant					
$L_{sr}$	Markstein length for strain	Greek sy	reek symbols			
$Ma_{sr}$	Markstein length for strain, $L_{sr}/\delta_l$	α	thermal diffusivity (m <sup>2</sup> /s) and coefficient constant			
n	power constant	β	coefficient constant			
P	pressure (MPa)	$\theta$	tip angle of the progress variable contour			
$P_0$	initial pressure (MPa)	$\delta_l$	laminar flame thickness (m)			
$P_e$	perimeter length of the turbulent flame contour; pressure	Ψ	sphericity			
	at the end of explosion (MPa)	χ	acceleration factor $(\overline{u}_{t,\overline{c}=0.5}/u_l)$			
$R_0$	diameter of the combustion vessel (190 mm)	$\nu$	unburned gas kinematic viscosity (m²/s)			
$r_{sch}$	flame front radius obtained by high-speed schlieren system (mm)	λ	Taylor length scale (m), $\lambda = L \left(\frac{16}{R_L}\right)^{1/2}$			
$r_{\overline{c}=0.5}$	flame radius at $\overline{c} = 0.5$	η	Kolmogorov length scale			
$Re_T$	Reynolds number, $Re_T = (u'/u_l)/(r_{sch}/\delta_l)$	ρ	density (kg/m <sup>3</sup> )			
$Re_L$	Reynolds number based on <i>L</i> , $Re_L = \frac{u'L}{v}$	$\rho_u$	unburned gas density (kg/m³)			
$S_{sch}$	flame propagtion speed based on schlieren flame radius	$ ho_b$	burned gas density (kg/m³)			
	(m/s)	$\rho_{\overline{c}=0.5}$	density at the $\overline{c} = 0.5$ surface (kg/m <sup>3</sup> )			
$\overline{S}_{sch}$	mean flame propagation speed evaluated over $r_{sch} = 15-50$	$\sigma$	thermal expansion ratio, $\sigma = \rho_u/\rho_b$			
	mm (m/s)	$\phi$	equivalence ratio			

velocities (u') from 0.6 to 2.8 m/s. Their findings indicate that the turbulent flame propagation speed increases with flame radius and higher turbulence intensity significantly enhances the turbulent flame speed. Kitagawa et al. [12] assessed the effects of pressure and u' (0.8 and 1.59 m/s) on turbulent flames and found that increasing both pressure and u' enhances the turbulent burning velocity. Zhao et al. [13] studied the effects of molecular transport on turbulent flame propagation, with u'=0.89 and 2.66 m/s. They found that the molecular transport has a significant promotion on the turbulent burning velocity. Furthermore, Nguyen et al. [14] measured premixed lean hydrogen/air flames with u' being 1.6 and 4 m/s and observed that spherical flames exhibit self-similar propagation behavior.

Although high u' conditions (> 4 m/s) are ubiquitous in practical combustion systems, including combustion engines and some pre-DDT phenomena in hazard management [15], the turbulent flame dynamics at such conditions remains not well studied, possibly limited by fan speed and size constraints. Subject to higher turbulence intensities, hydrogen flames may transition out of the flamelet regime and enter the regime of distributed reaction zone, potentially resulting in altered flame structure and propagation. It also remains unclear whether turbulent hydrogen flames continue to exhibit self-similar propagation with high u'. Additionally, given that turbulent hydrogen flames span a wide range of effective Lewis numbers, high turbulence intensities may amplify differential diffusion effects, leading to modulated flame front behaviors. Therefore, the first objective of the present study is to investigate the flame propagation behavior of turbulent hydrogen/air flames at high turbulence intensities.

The correlations for turbulent flame have been extensively developed, which facilitate the prediction of burning rates or flame propagation speed under various turbulent conditions, incorporating different

parameters, e.g., Karlovitz stretch factor (K), Damköhler number (Da), and Reynolds number ( $Re_T$ ). These correlations, often derived from experimental data, are widely used as inputs in turbulent combustion models for both Large Eddy Simulations (LES) and Reynolds-Averaged Navier-Stokes (RANS) simulations, enabling predictions of turbulent flame propagation [16,17]. Several turbulent burning velocity correlations, along with the corresponding definitions of turbulent burning velocity are summarized in Table 1. It should be noted that the turbulent burning velocity defined in these studies is an apparent quantity, representing the combined effects of chemical reaction and turbulent entrainment of fresh reactants into the flame brush on the overall flame front propagation. Abdel-Gayed et al. [18] reported that the ratio of the turbulent to laminar burning velocity,  $u_t/u_t$ , is correlated with the ratio of  $u'/u_t$  and a Karlovitz stretch factor defined as  $K = (u'/\lambda)(\delta_t/u_t)$ . Here,

**Table 1** Turbulent burning velocity correlations in [18–21,23,24].

Study	Correlation	Definition of $u_t$
Abdel-Gayed et al. [18]	$u_t/u_l \sim u'/u_l$	$u_t = (dr_{sch}/dt)(\rho_b/\rho_u)$
Kobayashi et al. [19]	$u_t/u_l \sim [(u'/u_l)/(P/P_0)]^{0.38}$	$u_t = U \sin \left( \theta/2 \right)$
Bradley et al. [20]	$u_t/u_k' \sim 0.88 (KLe)^{-0.3}$	$u_t = (dr_{sch}/dt)(\rho_b/\rho_u)$
Bradley et al.	$u_t/u_{k^{'}}=U\sim \ lpha K^{eta}, \ lpha \  ext{and} \ eta \  ext{are}$	$u_t =$
[21]	function of $Ma_{sr}$ .	$\frac{(4/3)\pi R_0^3}{(P_e - P_0)} \frac{(\rho_u/\rho) dP/dt}{\sum 2\pi r_{sch}^2 (1 - \cos\alpha)}$
Chaudhuri et al. [23]	$(dr_{sch}/dt)/S_s \sim Re_T^{0.54}$	N.A.
Liu et al. [24]	$u_{t,c=0.5}/u' \sim Da^{0.5}$	$u_{t,\overline{c}} = 0.5 =$
		$(dr_{\overline{c}} _{=0.5}/dt)(\rho_b/\rho_{\overline{c}} _{=0.5})$

 $u_t$  is calculated as  $(dr_{sch}/dt)(\rho_b/\rho_u)$ , where  $r_{sch}=\sqrt{A/\pi}$  is the burned-area-equivalent flame radius, A is the projected burned area, and  $\rho_u/\rho_b$  is the unburned-to-burned density ratio. In the definition of K,  $\lambda$  is the Taylor length scale and  $u_l$  is the laminar burning velocity.

Kobayashi et al. [19] proposed the correlation:  $u_t$  / $u_l$  ~  $[(u'/u_l)/(P/P_0)]^{0.38}$  from stabilized Bunsen-type turbulent methane/air flames. In this case,  $u_t$  is defined as  $U \sin(\theta/2)$ , where U is the mean flow velocity at the nozzle outlet and  $\theta$  is the tip angle of the progress variable (c) contour. Bradley et al. [20] considered the Lewis number and stretch rate and proposed  $u_t/u_{k'} = 0.88(KLe)^{-0.3}$ , where  $u_{k'}$  is the effective r.m.s turbulent velocity. Later, based on extensive measurements, Bradley et al. [21] further derived a general U-K correlation to highlight strain rate Markstein number,  $Ma_{sr}$  effects on turbulent burning velocity: U = $u_t/u_{k'} = \alpha K^{\beta}$ , while constants  $\alpha$  and  $\beta$  are functions of the  $Ma_{sr}$ . In their analysis,  $u_t$  was derived from the pressure rise rate and the burned-area-equivalent flame radius measured from schlieren images [21]. The parameter  $Ma_{sr}$  is defined as the ratio of the strain-rate-based Markstein length,  $L_{sr}$  to the laminar flame thickness,  $\delta_l$  as described in [22]. Given the large uncertainties in hydrogen/air  $Ma_{sr}$  [9], this  $Ma_{sr}$ based correlation is of limited reliability for hydrogen.

Chaudhuri et al. [23] found that the development of spherical turbulent flames follows a half-power law. The evolution of normalized flame propagation speed from turbulent to laminar,  $\left( dr_{sch} / dt \right) / S_s$ , collapses onto a single power-law of the instantaneous turbulent flame Reynolds number,  $Re_T$ , as  $(dr_{sch}/dt)/S_s \sim Re_T^{0.54}$  for methane flames with a Lewis number close to unity, which indicates self-similar propagation. The Reynolds number is defined as  $Re_T = (u'/u_l)/(r_{sch}/\delta_l)$ , where  $S_s$  is the unstretched laminar flame speed. Liu et al. [24] incorporated the Damköhler number (Da) into a half-power law correlation, expressed as  $u_{t,\overline{c}=0.5}/u' \sim Da^{0.5}$ . Here  $u_{t,\overline{c}=0.5}$  denotes the turbulent burning velocity evaluated at the flame radius corresponding to the half-burning-surface location  $\bar{c} = 0.5$ , and is defined as  $u_{t,\bar{c}} = 0.5 = 0.5$  $(dr_{\overline{c}=0.5}/dt)(\rho_h/\rho_{\overline{c}=0.5})$ . Recently, Nguyen et al. [14] reported that the correlations from Kobayashi et al. [19], Chaudhuri et al. [23], and Liu et al. [24] can be improved by scaling effective Lewis number ( $Le_{eff}$ ) as a grouping parameter. This suggests that the Lewis number effects on turbulent combustion cannot be neglected. However, to the best of our knowledge, these correlations have been developed from a specific range of turbulence intensities, particularly at relatively low u', and hence their applicability beyond these ranges is unclear. Therefore, the second objective of the present study is to propose representative flame propagation velocity correlations for hydrogen/air mixtures applicable to a wide range of turbulence intensities, from low to high.

To achieve the above two objectives, we used the fan-stirred combustion vessel equipped with high-speed schlieren imaging system to measure turbulent flame propagation over a range of u' from 0 to 9 m/s and  $\phi$  from 0.5 to 1.5. New correlations were developed, considering K and  $Re_T/Le_{eff}$ . The novelty of this work lies in the measurement of turbulent hydrogen flames under full range of u' (1–9 m/s) conditions and development of correlations applicable for a wider range of turbulence intensities. The remainder of the manuscript is organized as follows: Section 2 describes experimental setup. In Section 3, the results on turbulent flame propagation and representative flame propagation velocity correlations are presented and discussed. The main findings are summarized in Section 4.

### 2. Experimental setup

Experimental studies of hydrogen/air turbulent premixed flames were conducted in the Leeds fan-stirred spherical combustion vessel, utilizing high-speed schlieren imaging system. Detailed specifications of the combustion vessel and schlieren system are provided in Ref. [7]. Briefly, the vessel has a 380 mm internal diameter and a volume of 30

**Table 2** Experimental conditions of hydrogen/air mixtures (T = 300 K, P = 0.1 MPa).

φ	<i>u'</i> (m/s)	<i>u<sub>l</sub></i> (m/s)	$Le_{eff}$	$\delta_l$ (mm)	$\delta_l/u_l({ m ms})$	$\sigma = \\ \rho_u/\rho_b$	T <sub>ad</sub> (K)	$ u(\times 10^{-5} \\ m^2/s) $
0.5	0, 1,	0.67	0.51	0.41	0.61	5.02	1646	1.88
0.7	3, 5,	1.41	0.69	0.34	0.24	5.96	2022	1.99
0.8	7, 9	1.88	0.83	0.33	0.18	6.37	2178	2.05
0.9		2.03	1.03	0.33	0.16	6.66	2306	2.10
1.0		2.35	1.46	0.33	0.14	6.85	2390	2.16
1.1		2.45	1.88	0.33	0.13	6.90	2402	2.21
1.2		2.64	2.01	0.32	0.12	6.84	2371	2.26
1.5		2.89	2.47	0.30	0.10	6.53	2249	2.41

liters. Optical access is provided by two opposing 150-mm-diameter quartz windows, and ignition is initiated by a centrally located spark plug. Turbulence is generated by four eight-bladed fans powered by 8 kW motors, arranged tetrahedrally, with independent speed controls accurate to  $\pm$  5 % to ensure uniform and isotropic turbulence in the vessel central region. The turbulent flows within the combustion vessel were quantified in a previous study [25] using Particle Image Velocimetry (PIV). It was observed that the u' (m/s) within the vessel increases linearly with the fan rotational speed, f (rpm), i.e.,

$$u' = 0.00124f. (1)$$

The pressure during combustion was measured using a Kistler 701A dynamic pressure transducer, mounted flush to the vessel inner wall. The signal was amplified and recorded by a Kistler 5007 charge amplifier at a 50 kHz sampling rate. Turbulent flame images were captured using schlieren photography with a tungsten lamp, two lenses, and a high-speed DANTEC SpeedSense 2640 camera at 20,000–60,000 fps. The resolution was 512  $\times$  512 pixels, with each pixel at 0.263 mm. Flame schlieren images were processed in MATLAB using a binarizing-thresholding technique to accurately capture the two-dimensional projection of the burned area, A and the flame contour. Following the approach in Refs. [11–14,16], the burned area-equivalent flame radius is defined as  $r_{sch} = \sqrt{A/\pi}$ . The turbulent flame speed on the burned side,  $S_{sch}$ , is calculated as  $dr_{sch}/dt$ . To ensure repeatability and quantify uncertainty, each condition was tested in three independent experiments.

The experimental conditions and key parameters for hydrogen/air mixtures in this study are outlined in Table 2. Measurements were conducted over a wide range of  $\phi$  (0.5–1.5) and u' (0–9 m/s) to investigate the effects of turbulence intensity on flame propagation across lean, stoichiometric, and rich conditions. The laminar burning velocity ( $u_l$ ) is defined by  $u_l = (\rho_b/\rho_u) S_s$ , where  $S_s$  is the unstretched laminar flame speed, obtained by linear extrapolation of the laminar flame propagation speed versus stretch rate to the point of zero stretch rate. Where  $\rho_u$  and  $\rho_b$  are the densities of the unburned and burned gases, respectively. The effective Lewis number ( $Le_{eff}$ ), ranging from 0.51 to 2.47, was evaluated using the weighted average of the Lewis numbers of the excess and deficient reactants, following Bechtold et al. [26] and Bouvet et al. [27]:

$$Le_{eff} = 1 + \frac{(Le_E - 1) + (Le_D - 1)A}{1 + A}.$$
 (2)

Where  $Le_E$  and  $Le_D$  are the Lewis numbers of the excess and deficient reactants, respectively and A is the mixture strength factor. This range of  $Le_{eff}$  enables the investigation of Lewis number effects on turbulent hydrogen flames. The flame thickness  $\delta_l$  was derived from the temperature profile across the flame and is defined as [28]:  $\delta_l = (T_{ad} - T_u)/(dT/dx)_{max}$ , where  $T_{ad}$  is the adiabatic flame temperature and  $T_u$  is the unburned gas temperature. The ratio  $\delta_l/u_l$  characteristic chemical reaction time across the flame thickness.

#### 3. Results and discussion

## 3.1. Flame morphology and combustion regime

Fig. 1 presents the high-speed instantaneous schlieren images of both laminar and turbulent expanding hydrogen/air flames, all at  $r_{sch}=50$  mm. The time stamp in each image represents the time elapsed since ignition. Each column (top to bottom) corresponds to an increasing  $\phi$  from 0.5 to 1.5, with  $Le_{eff}$  varying from 0.51 to 2.47. As  $\phi$  increases, the influence of differential diffusion tends to diminish due to the reduced role of fast-diffusing hydrogen in rich mixtures [8,9]. Each row (left to right) represents increasing turbulence intensity, with u' from 0 m/s (laminar) to 9 m/s demonstrating the effects of turbulence intensity on flame morphology.

For the laminar flames (first column) with  $\phi=0.5$  and 0.7, the flame front exhibits cellular structures and a wrinkled front due to thermal-diffusivity (TD) instability, as the  $Le_{eff}$  is less than unity, 0.51 and 0.69, respectively. This indicates that mass diffusivity is greater than thermal diffusivity, meaning the faster diffusion of hydrogen compared to heat can lead to localized variations in temperature and reaction rates [29]. Increasing  $\phi$  results in an increase in  $Le_{eff}$ , e.g., relatively smooth and spherical flames are seen at  $\phi=1$  and 1.5 corresponding to  $Le_{eff}=1.46$  and 2.47, respectively. A similar phenomenon was observed in Refs. [8,9].

For a fixed  $\phi$ , increasing the u' leads to progressively more wrinkled, cellular, and distorted flame surfaces. At  $\phi=0.5$ , when u'=1 m/s, the flame surface becomes moderately wrinkled, and with u'=3 m/s, more pronounced cellular structures emerge with a visibly distorted flame

front. With further increase to u' = 5 and 7 m/s, the flame develops finescale wrinkling and loses spherical symmetry, characterized by a broadened flame brush and intensified surface irregularity due to enhanced flame-turbulence interactions. At the maximum u' = 9 m/s, the flame exhibits the highly irregular morphology, featuring a highly contorted front and significant flame brush thickening, indicative of strong turbulence-chemistry coupling and an increased surface area. At a fixed u', the flame morphology is also strongly influenced by the equivalence ratio. As  $\phi$  decreases from 1.5 to 0.5, the flame shows increased surface wrinkling, distortion, and loss of symmetry. This trend is attributed to the reduction in  $u_l$ , which leads to a longer chemical time scale across the flame thickness, expressed as  $\delta_l/u_l$ . Consequently, the Karlovitz stretch factor (K) increases, and the stretching intensity imposed by turbulence becomes stronger, leading to more pronounced flame deformation. A second possible explanation is provided by Howarth et al. [30], which shows that for lean hydrogen flames with a low Lewis number, turbulence can be coupled with TD instability, further wrinkling the flame surface.

The degree of turbulent flame surface wrinkling can be quantified using sphericity,  $\psi$  defined as:

$$\psi = 4\pi A/P_e^2,\tag{3}$$

where  $P_e$  is the perimeter length of the turbulent flame envelope. The flame envelope is defined as the outermost visible flame boundary extracted from schlieren images, with the  $P_e$  calculated by summing the number of edge pixels along the envelope and multiplying by the pixel size.  $\psi=1$  indicates a perfectly spherical flame with no wrinkling, while  $\psi<1$  means wrinkling and/or distortion.

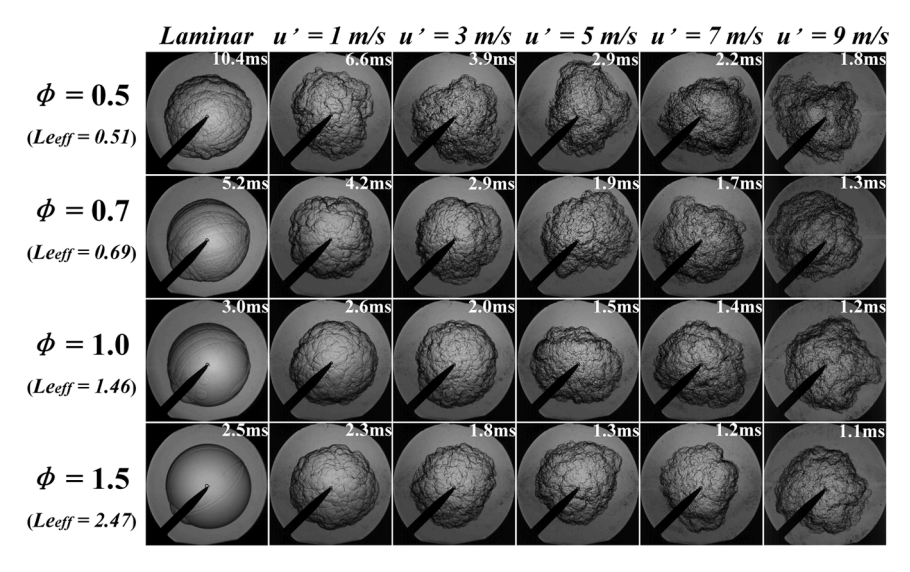


Fig. 1. schlieren images of hydrogen/air premixed flames with varying equivalence ratios  $\phi$  and turbulence intensities u'.

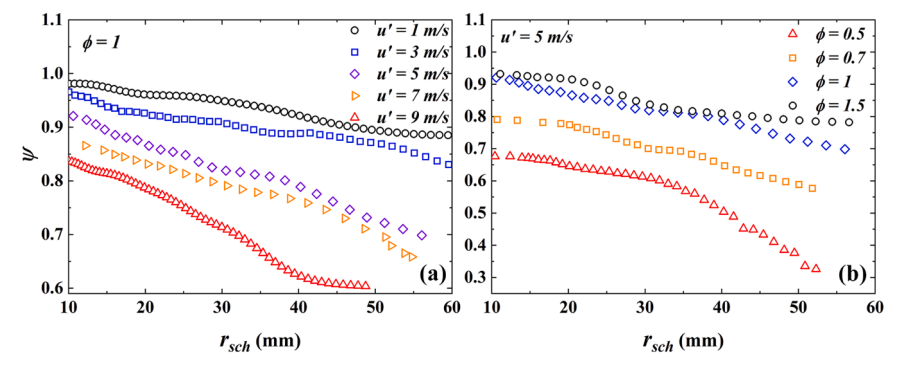


Fig. 2. Flame sphericity as a function of flame radius for hydrogen/air turbulent flames with different (a) turbulence intensities u' and (b) equivalence ratios φ.

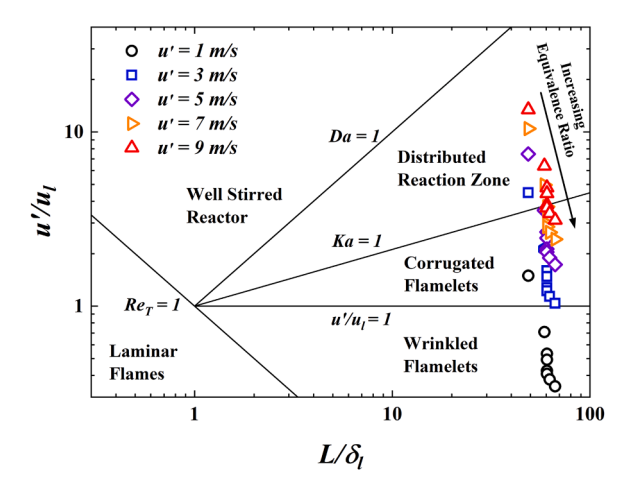


Fig. 3. Hydrogen/air premixed turbulent flame on Peters-Borghi [32] diagram.

Fig. 2 shows the change of turbulent flame sphericity with  $r_{sch}$ , highlighting the effects of u' in Fig. 2(a) and  $\phi$  in 2 (b). Generally, as the flame radius increases,  $\psi$  decreases non-linearly across all u' and  $\phi$ conditions, indicating increased flame wrinkling. This trend occurs because a larger radius encompasses a greater volume of turbulence, allowing more turbulent eddies to interact with and distort the flame front. In Fig. 2(a), increasing u' reduces the flame sphericity at all radii due to interactions with stronger, faster-moving turbulent eddies that disrupt the flame's sphericity. This is more evident at higher turbulent intensities ( $u' \ge 5$  m/s), where  $\psi$  decreases more significantly with  $r_{sch}$ , compared to the more gradual reduction at lower turbulent intensities (u' = 1 and 3 m/s). A similar trend was observed by Zhang et al. [31] in an IC engine, where higher engine speeds reduced flame sphericity. In contrast, Fig. 2(b) shows that at a fixed turbulence intensity (e.g., u'=5m/s), increasing  $\phi$  enhances flame sphericity with a lower degree of wrinkling. This trend is attributed to the increase in  $u_l$  at higher  $\phi$ , which reduces the chemical reaction time across the flame thickness (as shown in Table 1), thereby reducing the flame's exposure time to turbulent distortions.

Fig. 3 summarizes all our measurements in the Peters-Borghi diagram to classify turbulent combustion regimes. The integral length scale,

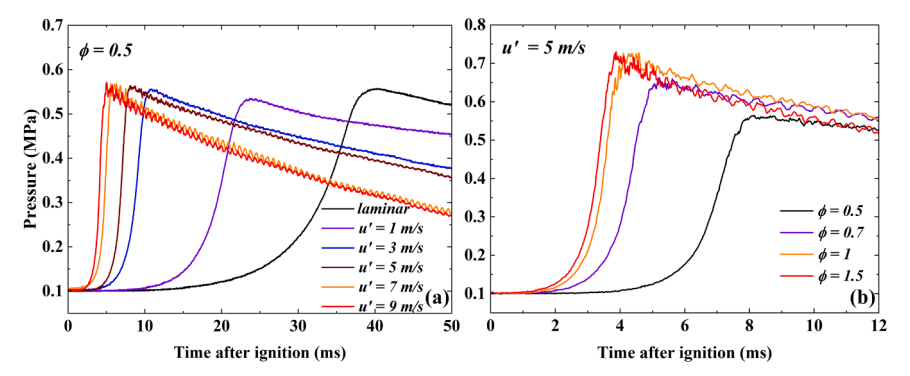


Fig. 4. Impact of (a) u' and (b)  $\phi$  on the pressure evolution of the combustion vessel.

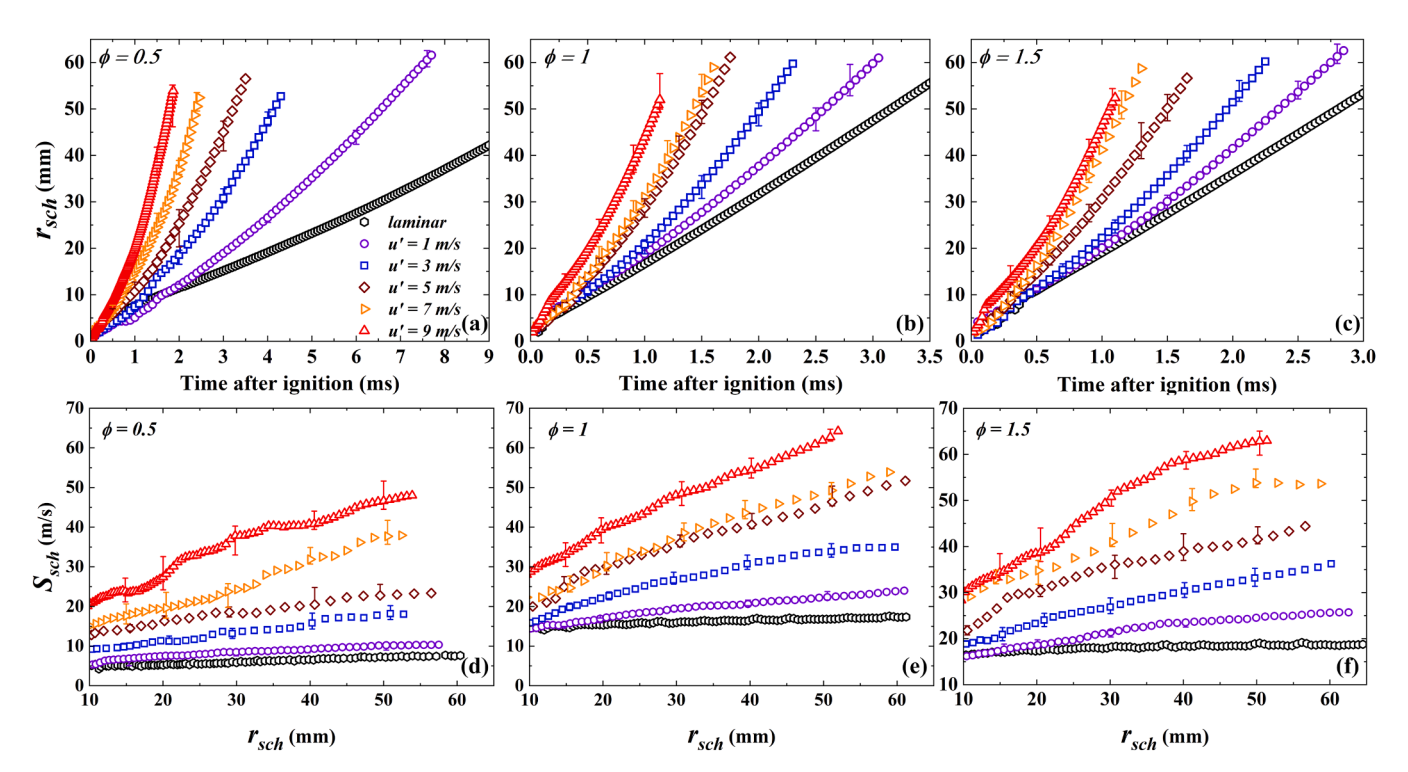


Fig. 5. Time history of flame radius,  $r_{sch}$ , and change of  $S_{sch}$  with  $r_{sch}$  at different turbulence intensities and equivalence ratios.

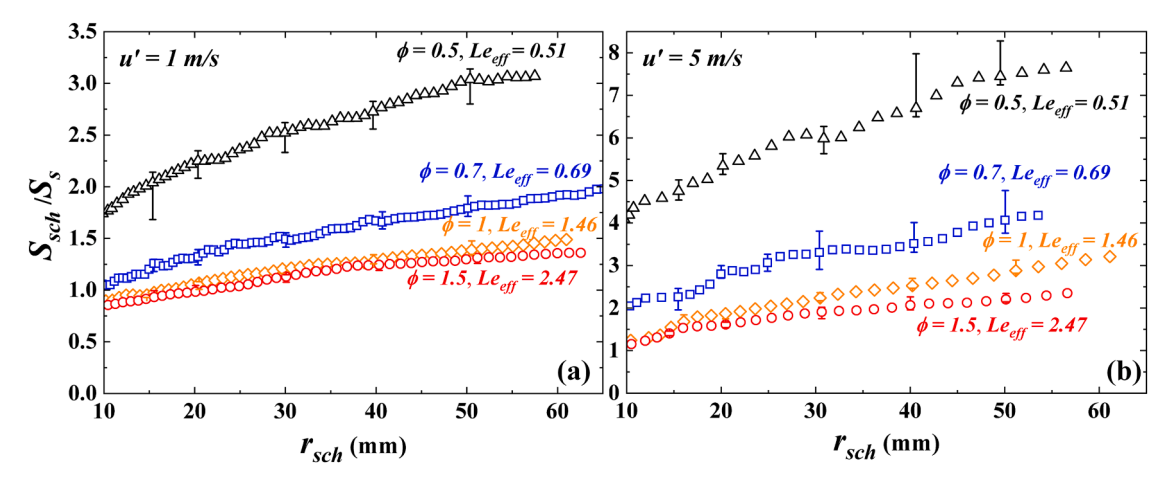


Fig. 6. Normalized turbulent flame speed,  $S_{sch}/S_s$ , against  $r_{sch}$  for increasing  $Le_{eff}$ .

L, within the combustion vessel is around 2 cm, based on the estimation in Ref. [25]. Increasing u' from 1 m/s to 9 m/s raises the  $u'/u_l$  ratio, causing the transition across various combustion regimes, including wrinkled flamelets, corrugated flamelets, and distributed reaction zones. For u' = 1 and 3 m/s, the data primarily fall within the flamelet regime, where the flame structure remains intact and the Karlovitz number *Ka* < 1. In this regime, the flame thickness is larger than the Kolmogorov scale, meaning it is embedded in eddies where the flow remains quasi-laminar, and small-scale turbulence is insufficient to disrupt the internal flame structure. At higher turbulent intensities (u' > 5 m/s), the data extend toward the distributed reaction zone, where Ka > 1. In this regime, the Kolmogorov scale becomes smaller than the flame thickness, allowing Kolmogorov-scale eddies to penetrate the flame and interact with its internal structure. Conversely, at a fixed u', increasing  $\phi$  can shift the distributed reaction zone back toward the flamelet zone. This is because increasing  $\phi$  raises  $u_l$  and decrease  $\delta_l$ , thereby reducing the  $u'/u_l$ ratio and increasing  $L/\delta_l$ , shifting the distribution towards the lower-right, as indicated by the arrow in Fig. 3.

# 3.2. Turbulence effect on pressure evolution

Fig. 4 shows the evolution of combustion chamber pressure during the flame propagation process. As depicted in Fig. 4(a), increasing u' from 0 to 9 m/s significantly shortens the time from ignition to peak pressure, reducing it from approximately 40 ms to 4 ms due to the enhanced burning rate. At higher turbulence intensity ( $u' \geq 5$  m/s), pressure oscillations appear after the pressure peak, with oscillation amplitude increasing as u' rises. Similarly, Fig. 4(b) shows that increasing  $\phi$  from 0.5 to 1.5 also shortens the ignition-to-peak interval and results in stronger pressure oscillations. The increasing amplitude of pressure oscillations is likely due to complex interactions between the turbulent flame and combustion vessel walls. Higher u' and  $\phi$  increase the burning rate and accelerate flame propagation, intensifying these interactions and generating acoustic waves that reflect within the chamber, thereby amplifying pressure oscillations [33].

# 3.3. Turbulent flame propagation speed

The evolutions of the area-equivalent flame radius,  $r_{sch}$ , are shown in Fig. 5(a), (b), and (c), which are respectively from the schlieren imaging at  $\phi=0.5, 1$  and 1.5. For each condition, three independent experiments were performed to assess repeatability and quantify experimental uncertainty. The error bars represent asymmetric uncertainties (upper and lower limits) derived from these three independent measurements at representative times and flame radii. In all cases,  $r_{sch}$  increase more rapidly over time as u' increases, primarily due to stronger flame

wrinkling caused by higher turbulence, which speeds up flame propagation. Fig. 5(d), (e), and (f) presents the flame propagation speed,  $S_{sch}$ , as a function of  $r_{sch}$  for various u' at  $\phi = 0.5$ , 1 and 1.5. For a fixed  $\phi$ , increasing u' leads to a rise in  $S_{sch}$  across all flame radii. The increase is not strictly linear and noticeable fluctuations occur, especially at u'=9m/s. Similar variations in turbulent flame propagation speed have also been reported in previous studies [13,16] Notably, at  $\phi = 1$ , the flame with u'=9 m/s exhibits an  $S_{sch}$  nearly three times greater than that u'=1m/s across the entire radius range, illustrating the strong influence of turbulence on flame acceleration. The magnitude of the errors also increases with u', indicating that uncertainty becomes more pronounced at higher turbulence intensities. The variation in error bar magnitude across flame radii indicates that measurement uncertainty is not constant during flame evolution. In all conditions,  $S_{sch}$  continues to increase with  $r_{sch}$  and no asymptotic or equilibrium propagation speed is observed, even as the flame expands beyond 60 mm.

The increase of  $S_{sch}$  with  $r_{sch}$  can be attributed to the progressive enhancement of flame surface wrinkling during flame expansion. Referring to Fig. 2, one can see that the flame sphericity continuously decreases with flame radius. This trend indicates enhanced flame wrinkling, which increases the flame front surface area and further accelerates the flame propagation speed. Abdel-Gayed et al. [18] and Bradley et al. [34] reported that a growing flame radius corresponds to an increase in turbulent flame surface density, resulting in greater flame front wrinkling. Chaudhuri et al. [23] further linked this acceleration to an increase in the hydrodynamic length scale and the growth of the turbulent flame brush thickness during flame propagation.

To quantify the turbulent effects on flame acceleration and eliminate the effects of laminar flame speed, the turbulent flame propagation speed,  $S_{sch}$ , is normalized by the unstretched laminar flame speed,  $S_s$ , as shown in Fig. 6(a) and (b) for u'=1 m/s and 5 m/s. Note that they correspond to different  $Le_{eff}$ . In both cases,  $S_{sch}/S_s$  increases with flame radius, but Fig. 6(b) shows a significantly greater enhancement, indicating stronger turbulent flame acceleration at higher turbulence intensities. Apparently, in both cases,  $S_{sch}/S_s$  increases as  $Le_{eff}$  decreases, indicating that hydrogen/air mixtures with low  $Le_{eff}$  experience enhanced turbulent flame acceleration. This may result from the combined effects of TD instability and turbulent eddies wrinkling the flame surface, which together accelerate turbulent flame propagation. Numerical studies by Howarth et al. [30], Aspden et al. [35], and Berger et al. [36] have demonstrated that the coupling between turbulence and TD instability significantly modifies flame structure and propagation characteristics. Specifically, turbulence amplifies the TD response by folding the flame surface, increasing the positive curvature, which enhances preferential diffusion.

Chaudhuri et al. [23] reported that flames with a near-unity Lewis

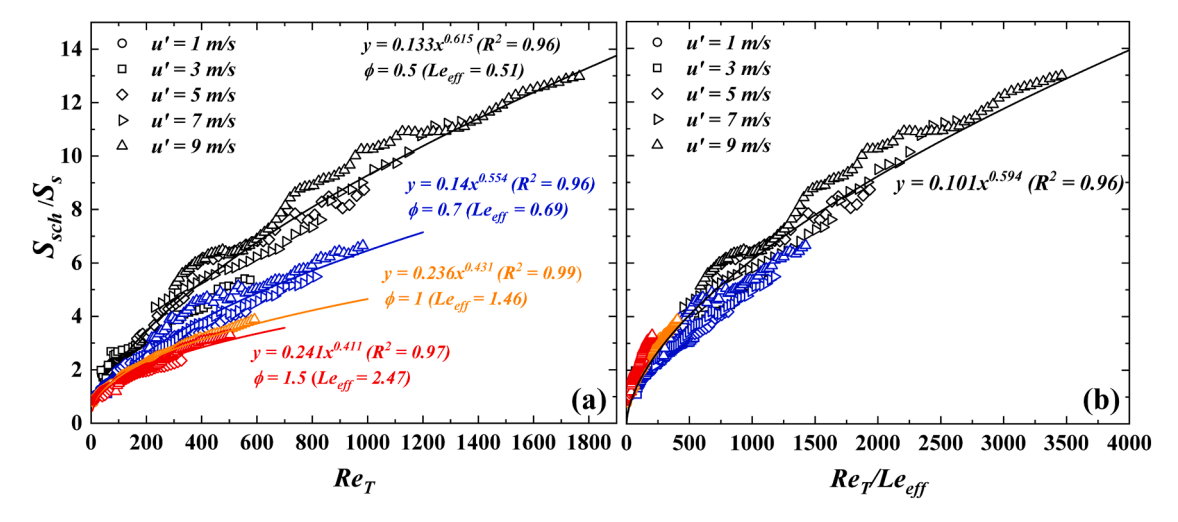


Fig. 7. Normalized  $S_{sch}/S_s$  against  $Re_T$  for increasing  $Le_{eff}$ , with u' from 1 to 9 m/s in (a) and against with  $Re_T/Le_{eff}$  in (b). Symbols represent experimental measurements, while solid lines depict best-fit correlations.

number exhibit self-similar flame propagation, where  $S_{sch}$  / $S_s$  scales with the Reynolds number  $Re_T = (u'/u_l)/(r_{sch}/\delta_l)$ . This Reynolds number depends on the flame radius and, in turbulent combustion, is hypothesized to scale with the hydrodynamic length scale of the flame surface fluctuations, which is assumed to be linearly proportional to  $r_{sch}$  [23]. The correlation follows a power law:

$$S_{\rm sch}/S_{\rm s} = \alpha Re_{\rm T}^{\beta}. \tag{4}$$

A research gap remains regarding whether self-similar flame propagation occurs in hydrogen/air mixtures with non-unity Lewis numbers under high u' condition. Fig. 7(a) shows  $S_{sch}/S_s$  plotted against  $Re_T$  for various  $Le_{eff}$  values during the turbulent flame propagation, with data corresponding to five levels of u'. For different  $Le_{eff}$ , distinct best-fit correlations are observed, regardless of u'. The power coefficient  $\beta$  does not remain constant at 0.5, as suggested by Chaudhuri et al. [23], but instead increases as  $Le_{eff}$  decreases. This suggests that the power-law expression in Eq. (4) is independent of u', but it does not universally apply across mixtures with different  $Le_{eff}$ . Nguyen et al. [14] and Wang et al. [37] have reported that the power-law correlation can be improved by normalizing  $Re_T$  with  $Le_{eff}$ , thereby accounting for Lewis number effects. Accordingly, the data in Fig. 7(a) are replotted against  $Re_T$  / $Le_{eff}$  in Fig. 7(b), where all points collapse well onto a single fitted curve with  $\beta=0.594$  and a coefficient of determination  $R^2$  value of 0.96.

# 3.4. Representative flame propagation velocity

The strict definition of turbulent burning velocity corresponds only to the chemical consumption of the fresh mixture and, by definition, should not include the turbulent entrainment of reactants into the flame brush. However, this quantity remains extremely challenging to obtain experimentally from schlieren measurements. In the present study, we therefore introduce a representative flame propagation velocity, which provides a quantitative measure of flame propagation and illustrates the effects of turbulence-induced acceleration. Owing to the wrinkled surface of a turbulent flame front, it is natural to evaluate the propagation velocity at a reference flame radius corresponding to a mean progress variable  $\overline{c}$ , where  $\overline{c} = 1$  denotes burned gas and  $\overline{c} = 0$  denotes unburned gas. Prior work [24] has shown that selecting  $\overline{c} = 0.5$  (the half-burning surface) provides a more representative velocity across different flame geometries, yielding good agreement between Bunsen-type and spherical flames. This definition has been adopted in several studies [14,16, 23,38]. Following the formulations of Bradley et al. [39] and Chaudhuri et al. [23], the representative flame propagation velocity at  $\bar{c} = 0.5$ , denoted  $u_{\bar{c}=0.5}$ , can be expressed in terms of the schlieren flame radius

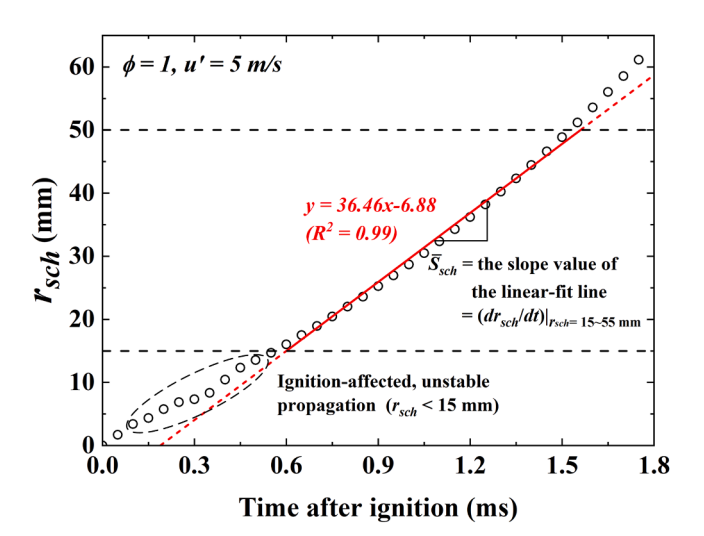


**Fig. 8.** Typical variation of flame radius with time, showing the determination of the mean turbulent flame propagation speed.

as:

$$u_{\bar{c}=0.5} = (\rho_b / \rho_{\bar{c}=0.5}) (dr_{sch} / dt) (r_{sch} / r_{\bar{c}=0.5})^2, \tag{5}$$

Where  $\rho_{\overline{c}=0.5}$  is the local density at  $\overline{c}=0.5$ , and  $r_{sch}/r_{\overline{c}=0.5}$  accounts for the offset between the schlieren radius and the half-burning surface. The density correction  $\rho_b/\rho_{\overline{c}=0.5}$  ensures consistency with mass conservation across the flame front. Experimental studies by Smallwood et al. [40] reported that the ratio of  $r_{sch}/r_{\overline{c}=0.5}$  is between 1.2 to 1.5 and Bradley et al. [39] reported that the ratio is between 1.3 to 1.5. In the present study, we adopt an empirical correction factor a for  $r_{sch}/r_{c=0.5}$ , with a=1.4, which corresponds to the representative average value of 1.3–1.5, to estimate the  $u_{\overline{c}=0.5}$ . Regarding the density at the half-burning surface,  $\rho_{\overline{c}=0.5}$ , Chaudhuri et al. [23] estimate  $\rho_{\overline{c}=0.5}=\frac{\rho_u+\rho_b}{2}$ , assuming an approximately linear variation between unburned and burned gases. Substituting these values into Eq. (5) yields:

$$u_{\bar{c}=0.5} = \left(\frac{2}{\sigma+1}\right) (dr_{sch} / dt) (1.4)^2 \tag{6}$$

where,  $\sigma = \frac{\rho_u}{\rho_b}$  is the thermal expansion ratio.

Since  $dr_{sch}/dt$  increases with  $r_{sch}$  and exhibits fluctuations (see Fig. 5), it is more appropriate to define a mean representative flame propagation

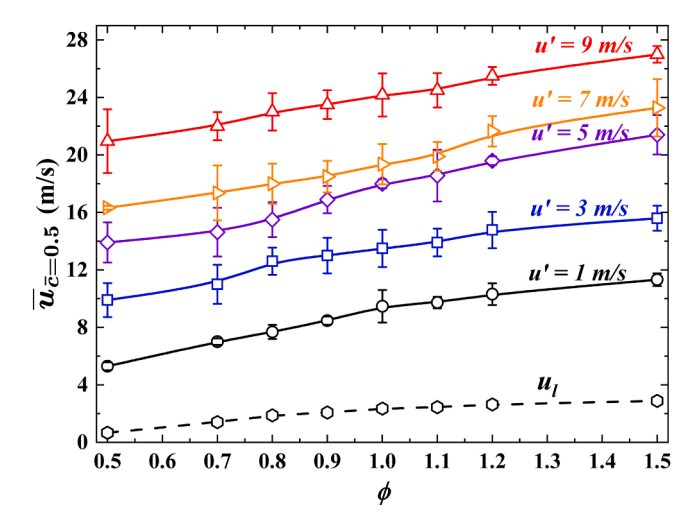


**Fig. 9.** Change of  $\overline{u}_{c=0.5}$  and  $u_l$  with  $\phi$  considering increased u'.

velocity,  $\overline{u}_{\overline{c}=0.5}$  over a selected flame radius range to enable quantitative comparison under different conditions. On this basis, Eq. (6) is reformulated as:

$$\overline{u}_{\tilde{c}=0.5} = \left(\frac{2}{\sigma+1}\right) (\overline{S}_{sch}) (1.4)^2 \tag{7}$$

where,  $\overline{S}_{sch}$  is the mean turbulent flame propagation speed evaluated in the flame radius range of  $r_{sch}=15$ –50 mm. Previous studies by Chen et al. [41] and Burke et al. [42] reported that, for spark-ignited flames, the early stage is strongly influenced by residual spark energy, leading to unstable flame propagation. A radius of about 15 mm is therefore sufficient to avoid residual spark effects, as also illustrated in Fig. 8, where  $r_{sch}<15$  mm corresponds to ignition-affected unstable propagation. At the other end, 50 mm is chosen because the flame is still free from chamber confinement, while in some cases larger flames may become distorted and even touch the optical window, making them unobservable. Following the approach of Liu et al. [24],  $\overline{S}_{sch}$  is determined by applying a best-fit linear regression to the flame radius-time history in the range  $r_{sch}=15$ –50 mm (illustrated in Fig. 8), with the slope of the fit taken as  $\overline{S}_{sch}$ .

Shown in Fig. 9, both  $u_l$  and  $\overline{u}_{\overline{c}=0.5}$  are averaged over three independent measurements, with error bars representing the standard deviation. For the hydrogen/air mixtures,  $\overline{u}_{\overline{c}=0.5}$  increases with both  $\phi$  and

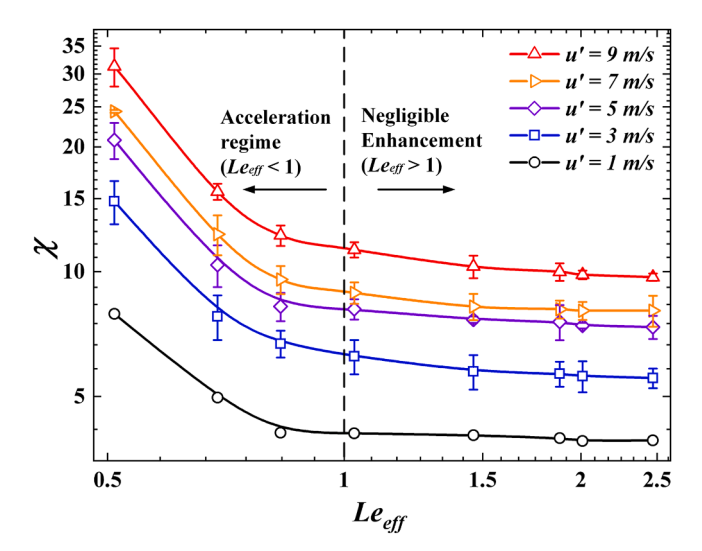


Fig. 10. Turbulent acceleration factor  $\chi$  versus  $Le_{eff}$  with different u'.

u', reaching a maximum of approximately 27 m/s at u' = 9 m/s and  $\phi =$ 1.5. This trend is consistent with that of  $u_l$ . The uncertainty also becomes significant when  $u' \geq 3$  m/s. To eliminate the influences of  $u_l$  and further explore the effects of  $Le_{eff}$  on  $\overline{u}_{\overline{c}=0.5}$ , the normalized acceleration factor  $\chi = \overline{u}_{\overline{c}=0.5}/u_l$  is plotted against  $Le_{eff}$  on a log-log scale for increasing u' in Fig. 10. It can be observed that, for all values of u', increasing  $Le_{eff}$  up to unity leads to a pronounced decrease in  $\chi$ , which corresponds to the acceleration regime. This suggests that at low Leeff, thermo-diffusive effects dominate the turbulent flame acceleration. In contrast, when  $Le_{eff} \geq 1$ , further increases in  $Le_{eff}$  only results in a negligible reduction in  $\chi$ , which we denote as the negligible enhancement regime. Because, as Leeff exceeds unity, preferential diffusion no longer amplifies flame front instabilities, and turbulent flame propagation becomes governed primarily by hydrodynamic turbulence-flame interactions rather than diffusion imbalance. Similar behavior was reported by Zhao et al. [13] for hydrogen/air spherical turbulent flames over a wide range of  $\phi$  (from 0.4 to 5.0) with corresponding Lewis numbers spanning from 0.42 to 4.06.

# 3.5. Correlation for the representative flame propagation velocity

Two representative flame propagation velocity correlations are presented in this study using both the present experimental data and literature data [12–14] for hydrogen/air turbulent flames in a fan-stirred combustion vessel. The dataset includes the measurements from Kitagawa et al. [12] for  $\phi$  from 0.4 to 1.0 with u'=0.8 m/s and 1.59 m/s, Zhao et al. [13] for a broader range of  $\phi$  from 0.4 to 5.0 with u'=0.8 m/s and 2.7 m/s, and Nguyen et al. [14] for  $\phi=0.6$  with u'=1.6 m/s and 4 m/s. For consistency, the literature data were converted to Eq. (7) to align with the present measurements. The first correlation is modified from the framework of Bradley's *U-K* correlation [21], and highlights the influence of the Karlovitz stretch factor (K) in characterizing the interaction between the mean flame propagation velocity ( $\overline{u}_{\overline{c}=0.5}$ ) and turbulence intensity (u'). It is expressed as:

$$\frac{\overline{u}_{\overline{c}=0.5}}{u'} = \alpha K^{\beta} = \alpha [(u'/\lambda)(\delta_l/u_l)]^{\beta}. \tag{8}$$

The Taylor microscale,  $\lambda$ , can be estimated as [43]:

$$\lambda = 4(u^{'-0.5}L^{0.5}\nu^{0.5}),\tag{9}$$

where  $\nu$  is the kinematic viscosity of the hydrogen/air mixture. The coefficient  $\alpha$  and  $\beta$  are empirical constants determined by fitting the experimental data.

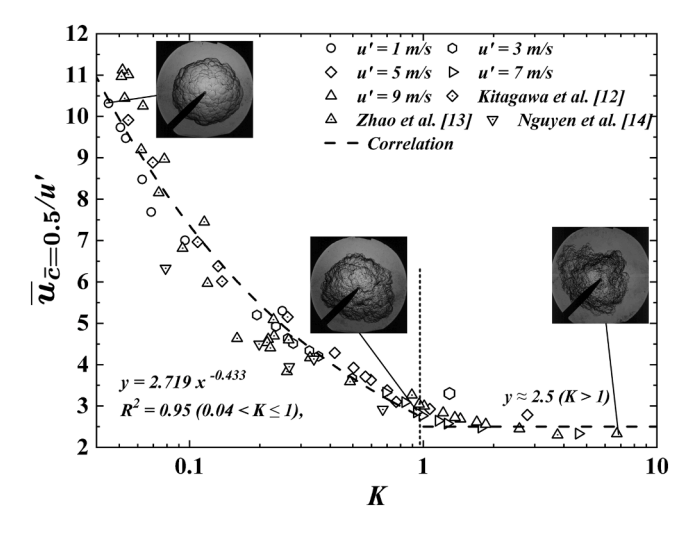


Fig. 11. Variation of  $\overline{u}_{\overline{c}=0.5}/u'$  with K for hydrogen/air turbulent flames at 300 K and 0.1 MPa.

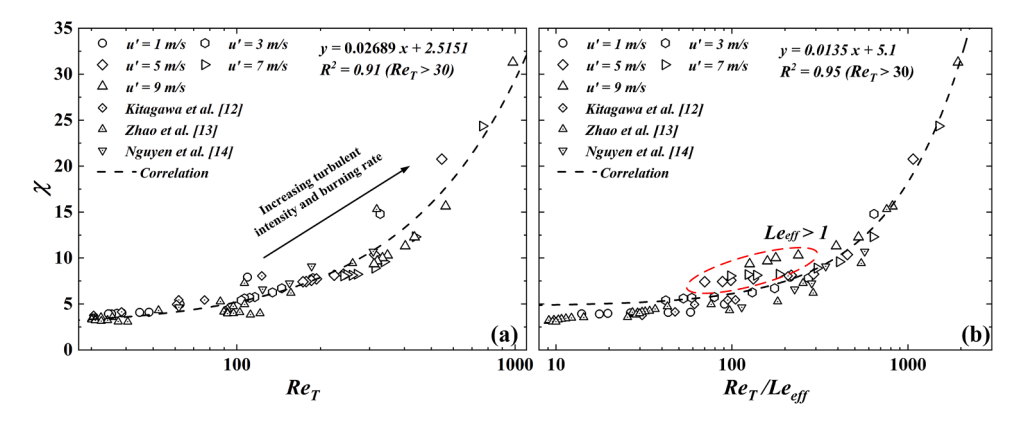


Fig. 12. Variation of  $\chi$  with  $Re_T$  in (a) and  $Re_T/Le_{eff}$  in (b) for hydrogen/air at 300 K and 0.1 MPa.

Fig. 11 illustrates the relationship between  $\overline{u}_{\overline{c}=0.5}/u'$  and K. Several factors influence the magnitude of K: as shown in Eq. (8), an increase in u' raises K, and according to Eq. (9), this increases in u' also reduces  $\lambda$ , further elevating K. Additionally, an increase in  $\phi$  for hydrogen/air enhances  $u_l$  resulting in a decrease in K. Fig. 11 shows that the ratio  $\overline{u}_{\overline{c}=0.5}/u'$  decreases as u' increases, suggesting that the rise in  $\overline{u}_{\overline{c}=0.5}$  is proportionally smaller than the increase in u' in the regime where K < 1. In this regime, the experimental data closely follow a power-law scaling and can be well represented by the correlation:  $\overline{u}_{\overline{c}=0.5}/u' = 2.719K^{-0.433}$  for K ranging from 0.04 to 1, achieving an excellent fit with an  $R^2$  of 0.95. When K exceeds unity, further increases in K cause  $\overline{u}_{\overline{c}=0.5}/u'$  to approach a nearly constant value of approximately 2.5.

The second correlation is based on the framework of Chaudhuri et al. [23] which considers the turbulent flame Reynolds number  $(Re_T)$  effects on the acceleration factor  $\chi = \overline{u}_{\overline{c}=0.5}/u_l$ . Fig. 12(a) illustrates that  $\chi$  increases with ReT, and the measured data follows a linear trend, well described by the correlation:  $\chi = 0.02689Re_T + 2.5151$  for  $Re_T$  from 30 to 980, achieving an  $R^2$  value of 0.91. It is noteworthy from Fig. 10 that differential diffusion significantly affects  $\chi$  particularly at low  $Le_{eff}$ . The study by Nguyen et al. [14] suggested that  $\chi$  is related to scaling of  $Le_{eff}^{n}$ , where n is the power constant and possible between 0.3 and 2. After multiple attempts to improve the correlation, the best fit was obtained by rescaling  $Re_T$  with  $Le_{eff}$  are shown in Fig. 12(b). Compared to Fig. 12 (a), incorporating the  $Le_{eff}$  scaling causes the data points to collapse onto a single linear trend, yielding the revised correlation:  $\chi = 0.0135 Re_T$  $/Le_{eff}+5.1$  with  $R^2$  improved to 0.95. However, some data points, highlighted within the red dashed circle in Fig. 12(b), deviate from the correlation. These outliers correspond to the cases where  $Le_{eff} > 1$  and u'> 5 m/s. Referring to Fig. 10, as the  $Le_{eff}$  large than unity, its influence on  $\chi$  diminishes, leading to an almost constant value of  $\chi$  with  $Le_{eff}$ . Consequently, applying the  $Le_{eff}$  scaling may not be effective for cases with  $Le_{eff} > 1$  and under high u' conditions.

#### 4. Conclusions

This study investigated the premixed turbulent hydrogen/air flames across a wide range of equivalence ratios from 0.5 to 1.5 and r.m.s turbulent velocity from 1 to 9 m/s using the fan-stirred combustion vessel with high-speed schlieren imaging. Emphasis is placed on the effects of turbulence intensity and effective Lewis number on turbulent flame propagation characteristics. The present measurements, combined with existing data from literature, were used to develop correlations for representative flame propagation velocity in hydrogen/air mixtures. The key findings are as follows:

- The present measurements span the wrinkled flamelet, corrugated flamelet, and distributed reaction zone regimes on the Peters-Borghi diagram. Pressure oscillations were observed in hydrogen/air flames after the peak pressure when u' higher than 5 m/s. The amplitude of pressure oscillations increased with both  $\phi$  and u'. The combustion duration, defined as the time from ignition to peak pressure, was found to decrease with increasing  $\phi$  and u', indicating an increased burning rate.
- Hydrogen/air turbulent flames exhibit self-similar propagation regardless of u', but this behavior is not maintained across different  $Le_{eff}$  values within the range  $0.51 < Le_{eff} < 2.47$ . Normalizing  $Re_T$  by  $Le_{eff}$  accounts for Lewis number effect and yields a unified correlation.
- The mean representative flame propagation velocities,  $\overline{u}_{\overline{c}=0.5}$ , for hydrogen/air flames increase with both  $\phi$  and u'. The maximum  $\overline{u}_{\overline{c}=0.5}$  was observed to reach approximately 27 m/s at u'=9 m/s and  $\phi=1.5$ . Meanwhile, the acceleration factor  $\chi=\overline{u}_{\overline{c}=0.5}/u_l$  varies across two distinct regimes with respect to  $Le_{eff}$ . For  $Le_{eff}<1$ , turbulent flame acceleration is strongly influenced by the thermodiffusive effects. In contrast, when  $Le_{eff}>1$ , flame propagation is governed primarily by hydrodynamic turbulence-flame interactions

# **Novelty and Significance**

The novelty of this research lies in the comprehensive measurement of premixed turbulent flame characteristics for expanding hydrogen/air flames under high r.m.s. turbulent velocities, up to 9 m/s, and across a wide range of equivalence ratios, using a fan-stirred combustion vessel. This study demonstrates that turbulent hydrogen flames exhibit self-similar propagation behavior, independent of u'. Additionally, the measured mean representative flame propagation velocity, along with existing data from the literature, is found to correlate well with K and  $Re_T/Le_{eff}$ , covering a wide range of  $Le_{eff}$  and u'. The significance of this research lies in its contribution to advancing the fundamental understanding of premixed turbulent hydrogen combustion, which is critical for the development of hydrogen-based combustion systems. Furthermore, the proposed correlations serve as important input parameters for advanced turbulent combustion modeling, with direct relevance to the development and optimization of hydrogen-fueled gas turbine systems.

- rather than diffusion imbalance, and  $\chi$  gradually approaches a constant value.
- The first proposed correlation considers the effect of Karlovitz stretch factor K in the regime where K < 1 and follows  $\overline{u}_{\overline{c}=0.5} / u' = 2.719 \ K^{-0.433}$ . In the regime where K > 1, the ratio  $\overline{u}_{\overline{c}=0.5} / u'$  stabilizes at approximately 2.5. The second correlation accounts for the effect of  $Re_T$  on  $\chi$ . When  $Re_T$  is normalized by  $Le_{eff}$ , the data follows a linear trend:  $\chi = 0.0135 Re_T / Le_{eff} + 5.1$ . However, this scaling becomes less effective for  $Le_{eff} > 1$  and u' > 5 m/s, where the effect of the Lewis number diminishes.

# CRediT authorship contribution statement

**Jinzhou Li:** Writing – original draft, Visualization, Investigation, Formal analysis. **Huangwei Zhang:** Writing – review & editing, Investigation. **Junfeng Yang:** Writing – review & editing, Supervision, Investigation, Conceptualization.

#### Declaration of competing interest

The authors declare that they have no known competing financial interests or personal relationships that could have appeared to influence the work reported in this paper.

### Acknowledgements

Dr. Junfeng Yang thanks EPSRC (Grant No EP/W002299/1) for the financial support. Dr. Jinzhou Li acknowledges Shell Global Solution Ltd. (UK) to partially support the PhD study. Dr. Huangwei Zhang is supported by Singapore's National Research Foundation under Low-Carbon Energy Research (LCER) Programme (U2305D4002). Authors would like to acknowledge the valuable discussions with Prof. Derek Bradley.

# Supplementary materials

Supplementary material associated with this article can be found, in the online version, at doi:10.1016/j.combustflame.2025.114521.

#### References

- A.L. Sánchez, F.A. Williams, Recent advances in understanding of flammability characteristics of hydrogen, Prog. Energy Combust. Sci. 41 (2014) 1–55.
- [2] S.J.M. Algayyim, K. Saleh, A.P. Wandel, I.M.R. Fattah, T. Yusaf, H.A. Alrazen, Influence of natural gas and hydrogen properties on internal combustion engine performance, combustion, and emissions: a review, Fuel 362 (2024) 130844.
- [3] D. Lou, X. Rao, Y. Zhang, L. Fang, P. Tan, Z. Hu, Investigation of impacts of hydrogen injection and spark strategy on knock in hydrogen engine, Int. J. Hydrogen Energy 82 (2024) 1252–1262.
- [4] S. Taamallah, K. Vogiatzaki, F.M. Alzahrani, E.M.A. Mokheimer, M.A. Habib, A. F. Ghoniem, Fuel flexibility, stability and emissions in premixed hydrogen-rich gas turbine combustion: technology, fundamentals, and numerical simulations, Appl. Energy 219 (2018) 511–547.
- [5] D. Cecere, E. Giacomazzi, A. Di Nardo, G. Calchetti, Gas turbine combustion technologies for hydrogen blends, Energies 16 (2023) 6829.
- [6] V.N. Gamezo, T. Ogawa, E.S. Oran, Numerical simulations of flame propagation and DDT in obstructed channels filled with hydrogen-air mixture, Proc. Combust. Inst. 31 (2007) 2463–2471.
- [7] J. Li, Y. Xie, M.E. Morsy, J. Yang, Laminar burning velocities, Markstein numbers and cellular instability of spherically propagating ethane/hydrogen/air premixed flames at elevated pressures, Fuel 364 (2024) 131078.
- [8] Y. Xie, M.E. Morsy, J. Li, J. Yang, Intrinsic cellular instabilities of hydrogen laminar outwardly propagating spherical flames, Fuel 327 (2022) 125149.

- [9] D. Bradley, M. Lawes, K. Liu, S. Verhelst, R. Woolley, Laminar burning velocities of lean hydrogen-air mixtures at pressures up to 1.0 MPa, Combust. Flame 149 (2007) 162–172.
- [10] J. Pareja, H.J. Burbano, Y. Ogami, Measurements of the laminar burning velocity of hydrogen-air premixed flames, Int. J. Hydrogen Energy 35 (2010) 1054–1060.
- [11] J. Goulier, A. Comandini, F. Halter, N. Chaumeix, Experimental study on turbulent expanding flames of lean hydrogen/air mixtures, Proc. Combust. Inst. 36 (2017) 1523–1530.
- [12] T. Kitagawa, T. Nakahara, K. Maruyama, K. Kado, A. Hayakawa, S. Kobayashi, Turbulent burning velocity of hydrogen-air premixed propagating flames at elevated pressures, Int. J. Hydrogen Energy 33 (2008) 7452–7458.
- [13] H. Zhao, G. Li, J. Wang, Z. Huang, Experimental study of H<sub>2</sub>/air turbulent expanding flames over wide equivalence ratios: effects of molecular transport, Fuel 341 (2023) 127652.
- [14] M.T. Nguyen, D.W. Yu, S.S. Shy, General correlations of high pressure turbulent burning velocities with the consideration of Lewis number effect, Proc. Combust. Inst. 37 (2019) 2391–2398.
- [15] V.L. Zimont, Gas premixed combustion at high turbulence. Turbulent flame closure combustion model, Exp. Therm. Fluid Sci. 21 (2000) 179–186.
- [16] X. Cai, J. Wang, Z. Bian, H. Zhao, M. Zhang, Z. Huang, Self-similar propagation and turbulent burning velocity of CH<sub>4</sub>/H<sub>2</sub>/air expanding flames: effect of Lewis number, Combust. Flame 212 (2020) 479–490.
- [17] J. Li, S. Van Loo, J. Yang, A. Pekalski, Turbulent flame acceleration and deflagration-to-detonation transitions in ethane–air mixture, Phys. Fluids 36 (2024) 036118.
- [18] R.G. Abdel-Gayed, K.J. Al-Kishali, D. Bradley, Turbulent burning velocities and flame straining in explosions, Proc. R. Soc. Lond. A 391 (1984) 393–414.
- [19] H. Kobayashi, K. Seyama, H. Hagiwara, Y. Ogami, Burning velocity correlation of methane/air turbulent premixed flames at high pressure and high temperature, Proc. Combust. Inst. 30 (2005) 827–834.
- [20] D. Bradley, A.K.C. Lau, M. Lawes, F.T. Smith, Flame stretch rate as a determinant of turbulent burning velocity, Philos. Trans. R. Soc. Lond. A 338 (1992) 359–387.
- [21] D. Bradley, M. Lawes, K. Liu, M.S. Mansour, Measurements and correlations of turbulent burning velocities over wide ranges of fuels and elevated pressures, Proc. Combust. Inst. 34 (2013) 1519–1526.
- [22] D. Bradley, P.H. Gaskell, X.J. Gu, Burning velocities, Markstein lengths, and flame quenching for spherical methane—air flames: a computational study, Combust. Flame 104 (1996) 176–198.
- [23] S. Chaudhuri, F. Wu, D. Zhu, C.K. Law, Flame speed and self-similar propagation of expanding turbulent premixed flames. Phys. Rev. Lett. 108 (2012) 044503.
- [24] C.C. Liu, S.S. Shy, M.W. Peng, C.W. Chiu, Y.C. Dong, High-pressure burning velocities measurements for centrally-ignited premixed methane/air flames interacting with intense near-isotropic turbulence at constant Reynolds numbers, Combust. Flame 159 (2012) 1561–1575.
- [25] D. Bradley, M. Lawes, M.E. Morsy, Measurement of turbulence characteristics in a large-scale fan-stirred spherical vessel, J. Turbul. 20 (2019) 195–213.
- [26] J.K. Bechtold, M. Matalon, The dependence of the Markstein length on stoichiometry, Combust. Flame 127 (2001) 1906–1913.
- [27] N. Bouvet, F. Halter, C. Chauveau, Y. Yoon, On the effective Lewis number formulations for lean hydrogen/hydrocarbon/air mixtures, Int. J. Hydrogen Energy 38 (2013) 5949–5960.
- [28] G. Jomaas, C.K. Law, J.K. Bechtold, On transition to cellularity in expanding spherical flames, J. Fluid Mech. 583 (2007) 1–28.
- [29] T. Zirwes, F. Zhang, T.L. Kaiser, K. Oberleithner, O.T. Stein, H. Bockhorn, A. Kronenburg, The role of thermodiffusion and dimensionality in the formation of cellular instabilities in hydrogen flames, Proc. Combust. Inst. 40 (2024) 2557–2565.
- [30] T.L. Howarth, E.F. Hunt, A.J. Aspden, Thermodiffusively-unstable lean premixed hydrogen flames: phenomenology, empirical modelling, and thermal leading points, Combust. Flame 253 (2023) 112811.
- [31] W. Zhang, M.E. Morsy, Z. Ling, J. Yang, Characterization of flame front wrinkling in a highly pressure-charged spark ignition engine, Exp. Therm. Fluid Sci. 132 (2022) 110534.
- [32] R. Borghi, D. Escudie, Assessment of a theoretical model of turbulent combustion by comparison with a simple experiment, Combust. Flame 56 (1984) 101–108.
- [33] D. Bradley, J. Li, Reaction propagation, leading to developing detonation, in a rapid compression machine, Combust. Flame 262 (2024) 113331.
- [34] D. Bradley, M. Lawes, M.S. Mansour, Flame surface densities during spherical turbulent flame explosions, Proc. Combust. Inst. 32 (2009) 359–366.
- [35] A.J. Aspden, M.S. Day, J.B. Bell, Turbulence-flame interactions in lean premixed hydrogen: transition to the distributed burning regime, J. Fluid Mech. 680 (2011) 287–320.
- [36] L. Berger, A. Attili, H. Pitsch, Synergistic interactions of thermodiffusive instabilities and turbulence in lean hydrogen flames, Combust. Flame 244 (2022) 112254.
- [37] S. Wang, A.M. Elbaz, G. Wang, Z. Wang, W.L. Roberts, Turbulent flame speed of NH<sub>3</sub>/CH<sub>4</sub>/H<sub>2</sub>/H<sub>2</sub>O/air mixtures: effects of elevated pressure and lewis number, Combust. Flame 247 (2023) 112488.
- [38] S.S. Shy, C.C. Liu, J.Y. Lin, L.L. Chen, A.N. Lipatnikov, S.I. Yang, Correlations of high-pressure lean methane and syngas turbulent burning velocities: effects of

- turbulent Reynolds, Damköhler, and Karlovitz numbers, Proc. Combust. Inst. 35 (2015) 1501–1509.
- [39] D. Bradley, M.Z. Haq, R.A. Hicks, T. Kitagawa, M. Lawes, C.G.W. Sheppard, R. Woolley, Turbulent burning velocity, burned gas distribution, and associated flame surface definition, Combust. Flame 133 (2003) 415–430.
- [40] G.J. Smallwood, Ö.L. Gülder, D.R. Snelling, B.M. Deschamps, I. Gökalp, Characterization of flame front surfaces in turbulent premixed methane/air combustion, Combust. Flame 101 (1995) 461–470.
- [41] Z. Chen, M.P. Burke, Y. Ju, Effects of Lewis number and ignition energy on the determination of laminar flame speed using propagating spherical flames, Proc. Combust. Inst. 32 (2009) 1253–1260.
- [42] M.P. Burke, Z. Chen, Y. Ju, F.L. Dryer, Effect of cylindrical confinement on the determination of laminar flame speeds using outwardly propagating flames, Combust. Flame 156 (2009) 771–779.
- [43] W.D. McComb, The Physics of Fluid Turbulence, Oxford University Press, 1992.